Quantum Dynamics simulations of Polariton Spectroscopy

Elious Mondal

June 12th, 2023
Oral Exam Location and Time: Hutchison 118, 1:00 pm - 3:00 pm

Thesis Advisoty Committee Members:

Pengfei Huo (advisor)

Todd Krauss
David McCamant

Contents

1 Abstract

In this proposal, I present my work on developing a path-integral based quantum dynamics method for simulating spectroscopy of polaritons. I present some preliminary linear absorption and 2D electronic spectra calculations of some simple polaritonic systems. I propose that this method can be efficiently used for simulating a large number of molecules coupled to the cavity, which can help in understanding processes like polaron decoupling and also help to probe the polariton dark-state dynamics. Furthermore, I plan to extend this work to vibrational polaritons.

2 Introduction

When molecules couple to the quantized radiation field inside an optical cavity, new hybrid light-matter states, called polaritons form. Due to this rich dynamical interaction among electronic and photonic degrees of freedom, one can control the curvature of the electronic potential energy curvature and efficiently control the chemical reactivity[1–5]. Recent experimentation has now demonstrated this collective coupling of large ensembles of molecules to an optical cavity, provides enhanced control over chemical reactions[6–8], and effectively decouples the system from its external bath (solvent) effects[7]. Understanding the spectroscopy of these polariton systems will pave the way toward unraveling the mysteries of polariton chemistry. In particular, 2D electronic spectroscopy (2DES) can reveal inherent intermolecular two-body couplings, where the broadening of peaks indicates the coupling of the bath to the system and the fluctuations of the intensity peaks give direct evidence of coherent mechanisms in the system[9–12]. Therefore, 2D spectroscopy is a very useful experimental technique for exploring polaritonic properties.

2.1 Linear Response Spectroscopy

The linewidth of any molecule can give us information about how the excited-state dynamics occurs and how the relaxation occurs, thus also giving a hint about the kind of environment in which a molecule is present. To obtain this spectrum, we can probe the dynamics by exciting the system at different frequencies and recording the relaxation process. We excite an ensemble of molecules, and each molecule responds by emitting radiation. Since each molecule experiences a slightly different environment, the signal emitted by a molecule in the ensemble has a slightly different frequency than the other molecules. The overall response is the ensemble average of radiation emitted from the coherence oscillations of each molecule, and because of the emission of radiation at different frequencies, the interference of these gives off a decaying coherent signal.

Under perturbation theory, linear absorption can be written as a dipole-dipole auto-correlation function with the ensemble averaging done over the ground state density matrix of the ensemble.[9–12]

$$R^{(1)}(t) = -i\langle\hat{\mu}(t_1)[\hat{\mu}(t_0), \hat{\rho}_g]\rangle. \tag{1}$$

Here, $\hat{\mu}(t_1)$ is the dipole operator in the interaction picture, $\hat{\rho}_g = \mathrm{Tr}_R[\hat{\rho}]$ represents the reduced density matrix of the quantum subsystem (by tracing out the nuclear DOF) in the equilibrium ground state at $t = -\infty$, ($\hat{\rho}_g = \hat{\rho}(-\infty)$) and $\langle ...\rangle$ represents trace over the system DOF (states). The frequency domain spectra can be computed from a Fourier transform of $R^{(1)}(t)$ as follows

$$R^{(1)}(\omega) = \int_0^T R^{(1)}(t)e^{i\omega t}\cos\left(\frac{\pi t}{2T}\right)\mathrm{d}t, \tag{2}$$

where T is the maximum time of recorded time domain spectra and $\cos(\pi t/2T)$ is a smoothening function. The linear spectra is often limited in the amount of information we can extract for a given system, such as distinguishing different broadening mechanisms arising due to homogeneous or inhomogeneous distribution of frequencies and the internal couplings driving the coherent mechanisms in the system.

This deficiency can be overcome by perturbing the system multiple times with consecutive laser pulses. Each additional laser pulse is an additional probing tool for different mechanisms in the system, which can be interpreted from different pathways in the Liouville space. Here, I focus on two-dimensional electronic spectroscopy which can reveal coherent energetic pathways in the electronic subsystem and also different broadening mechanisms due to the coupling of electronic subsystem to different phononic environment. For a general two-dimensional spectroscopy experiment, one uses three lasers with different time delays and thus the 3$^{\text{rd}}$ order response can be calculated from a four-point correlation function

$$R^{(3)}(t_1, t_2, t_3) = -i\langle\hat{\mu}(t_3)[\hat{\mu}(t_2), [\hat{\mu}(t_1), [\hat{\mu}(t_0), \hat{\rho}_g]]]\rangle, \tag{3}$$

Here, the factor of $-i$ comes from $(-i)^3$ in the third order of perturbative expansion. Furthermore, $R^{(3)}$ can be decomposed into 8 different Liouville pathways, each represents a separate Feynman diagram and gives rise to a non-linear response signal. Each of the response signals is also accompanied by a phase factor that makes it possible to have an independent spatial direction of detection for each diagram. All of these Liouville pathways (Feynman Diagrams) can be categorized as either rephasing or non-rephasing signals, based on the phase accumulated by the signal after the application of the third laser pulse. These signals can be further divided into three physical processes, namely, Simulated Emission (SE), Ground State Bleach (GSB), and Excited State Absorption (ESA). The first four Liouville pathways are

$$R_1^{(3)}(t_1, t_2, t_3) = -i\langle\hat{\mu}(t_3)\hat{\mu}(t_0)\hat{\rho}_g\hat{\mu}(t_1)\hat{\mu}(t_2)\rangle, \tag{4a}$$

$$R_2^{(3)}(t_1, t_2, t_3) = -i\langle\hat{\mu}(t_3)\hat{\mu}(t_1)\hat{\rho}_g\hat{\mu}(t_0)\hat{\mu}(t_2)\rangle, \tag{4b}$$

$$R_3^{(3)}(t_1, t_2, t_3) = -i\langle\hat{\mu}(t_3)\hat{\mu}(t_2)\hat{\rho}_g\hat{\mu}(t_0)\hat{\mu}(t_1)\rangle, \tag{4c}$$

$$R_4^{(3)}(t_1, t_2, t_3) = -i\langle\hat{\mu}(t_3)\hat{\mu}(t_2)\hat{\mu}(t_1)\hat{\mu}(t_0)\hat{\rho}_g\rangle, \tag{4d}$$

and the remaining four are just the complex conjugate of them. In purely-absorptive 2D experiments, the signal is calculated by adding the rephasing and non-rephasing signals as follows

$$R^{(3)}_{\mathrm{rep}}(t_1, t_2, t_3) = R^{(3)}_2 + R^{(3)}_3 + R^{(3)*}_1, \tag{5a}$$

$$R^{(3)}_{\mathrm{nrp}}(t_1, t_2, t_3) = R^{(3)}_1 + R^{(3)}_4 + R^{(3)*}_2. \tag{5b}$$

In Eq. 5a and Eq. 5b, the terms on the right-hand side are ordered SE, GSB and ESA, respectively. Note that the formalism presented below can be used to calculate all possible non-linear spectroscopy experiments and is not limited to just Eq. 5a and Eq. 5b. Usually, 2D spectra is represented as the imaginary part of t_2 varying series of the Fourier transformed t_1 and t_3 axis. Because of the rephasing (non-rephasing), the signals are generated in different quadrants of the frequency domain. As such, the 2D Fourier transfrom is done by

$$R^{(3)}_{\mathrm{rep}}(\omega_1, t_2, \omega_3) = \int_0^{T_1}\int_0^{T_3} R^{(3)}_{\mathrm{rep}} e^{i\omega_3 t_3 - i\omega_1 t_1} S_1 S_3 \mathrm{d}t_1 dt_3, \tag{6a}$$

$$R^{(3)}_{\mathrm{nrp}}(\omega_1, t_2, \omega_3) = \int_0^{T_1}\int_0^{T_3} R^{(3)}_{\mathrm{nrp}} e^{i\omega_3 t_3 + i\omega_1 t_1} S_1 S_3 \mathrm{d}t_1 \mathrm{d}t_3, \tag{6b}$$

where the smoothening function S_i is

$$S_i = \cos\left(\frac{\pi t_i}{2T_i}\right).$$

With Eq. 6a and Eq. 6b, we can now represent the conventional purely-absorptive 2D spectra,

$$R^{(3)}(\omega_1, t_2, \omega_3) = -\,\mathbb{I}\mathrm{m}(R^{(3)}_{\mathrm{rep}} + R^{(3)}_{\mathrm{nrp}}). \tag{7}$$

2.2 $\mathcal{L}$-PLDM Dynamics

Any diabatic hamiltonian of a quantum system under the influence of a bath (environment) can be expressed as,

$$\hat{H}_{\mathrm{S}}(R) = \frac{P^2}{2M} + \sum_{a}^{\mathcal{N}} V_{aa}(R)|a\rangle\langle a| + \frac{1}{2}\sum_{b\neq a}^{\mathcal{N}} V_{ab}(R)|a\rangle\langle b| \tag{8}$$

where R and P are the position and momenta of the bath coordinates and M is the mass of bath particles. As the total number of states, $\mathcal{N}$, increases, quantum dynamics simulations can become heavily expensive due to the exponential scaling[13–15] of the calculation with the number of degrees of freedom. To simulate ensemble properties of such big and complex systems where some quantum degrees of freedom (DOF) ($\{|a\rangle\}$) might be interacting with a large number of classical DOF's ($\{R\}$), we need to simulate the reduced density matrix of the quantum subsystem (or in principle any other operator in the quantum system subspace) which takes into account all the feedback from classical DOF's. To perform such operator dynamics, we use the Partial Linearized Density Matrix (PLDM) approach to calculate the reduced quantum subsystem operator dynamics. This approach maps the quantum states to a series of singly excited fictitious harmonic oscillators such that the mapped diabatic Hamiltonian becomes

$$\mathcal{H}(R) = \frac{P^2}{2M} + \frac{1}{2}\sum_{a} V_{aa}(R)(x_a^2 + p_a^2 - 1) + \frac{1}{2}\sum_{b\neq a} V_{ab}(R)(x_a x_b + p_a p_b). \tag{9}$$

where x_a and p_a are now the mapping variables for state $|a\rangle$. The electronic states now evolve with feedback from nuclear bath as,

$$\frac{\partial x_a}{\partial t} = \frac{\partial \mathcal{H}}{\partial p_a} = \frac{1}{\hbar}\sum_{b} V_{ab}(R)p_b, \tag{10a}$$

$$\frac{\partial p_a}{\partial t} = -\frac{\partial \mathcal{H}}{\partial x_a} = -\frac{1}{\hbar}\sum_{b} V_{ab}(R)x_b, \tag{10b}$$

Having described the dynamics of electronic subsytem under the influence of some phonon environment, we also need a treatment for evolution of photonic modes under the influence of photonic bath (for lossy cavities). This is achieved by Lindblad Master equation, where the evolution of a photonic subsystem ($\hat{\rho}_S$) in presence of a lossy environment is described by,

$$\frac{\partial \hat{\rho}_{\mathrm{S}}}{\partial t} = -\frac{i}{\hbar}[\hat{H}, \hat{\rho}_{\mathrm{S}}] + \sum_k \Gamma_k \left(\hat{L}_k \hat{\rho}_{\mathrm{S}} \hat{L}_k^\dagger - \frac{1}{2}\{\hat{L}_k^\dagger \hat{L}_k, \hat{\rho}_{\mathrm{S}}\} \right), \tag{11}$$

where the environment causes decay in the photonic subsystem through loss channels $\hat{L}_k$ with rate Γ_k. To describe polaritonic dynamics, PLDM has been combined with Lindblad dynamics in an approach similar to that described in Ref. 16 and we call it the $\mathcal{L}$-PLDM approach. With this combined approach, we can describe the combined electronic-photonic subsystem dynamics,

$$\hat{\rho}(t + \mathrm{d}t) = e^{\mathcal{L}_{\hat{L}} \mathrm{d}t/2} e^{\mathcal{L}_{\hat{H}} \mathrm{d}t} e^{\mathcal{L}_{\hat{L}} \mathrm{d}t/2} \hat{\rho}(t), \tag{12}$$

where $e^{\mathcal{L}_{\hat{L}}}$ is the photonic decay dynamics (Eq. 11) and $e^{\mathcal{L}_{\hat{H}}}$ is the PLDM propagation based on the system Hamiltonian (Eq. 10a, Eq. 10b).

3 Projects/Hypothesis

3.1 Simulating Polariton spectroscopy with $\mathcal{L}$-PLDM dynamics

The PLDM algorithm has been earlier shown to be very accurate in simulating linear and non-linear spectroscopy of big systems in complex molecular environments [13]. The non-perturbative nature of the algorithm makes the treatment extendable to arbitrary system bath coupling strengths and thus effectively capturing non-markovian bath feedback in reduced quantum system dynamics. The inclusion of Lindblad[16] treatment now gives us additional freedom of selectively treating different subsystems of a quantum system as either markovian or nor-markovian in the same dynamics. Thus, with $\mathcal{L}$-PLDM, we can now combine markovian

photonic dynamics and non-markovian electronic dynamics to simulate linear and non-linear spectroscopy of Polaritons. This approach can in principle be also extended to simulate spectroscopy for any general systems in which we want to specifically treat some quantum DOF's as Markovian and others as non-markovian.

3.2 Polaron Decoupling

Polaritons are large macroscopic states that involve a coherent superposition of excitations among a large number of molecules. Due to this extensive delocalization over a large number of molecules, the normal modes of individual molecules are now collectively shared between all molecules in the superposition, because of which the highly delocalized polaritonic wavefunction now becomes effectively decoupled from the collective normal mode of the whole ensemble. This feature can be directly observed by reduction of linewidth in linear spectra. Watanabe and Takahasi have experimentally observed[7] the collective decoupling of the polaritons from a quantum vibration via flattening of nodal angle of the lower polariton in 2DES due to easier spectral duffusion in the highly delocalized polaritonic wavefunction. Simulation of polaron decoupling can help us develop effective polariton-bath models and also better understand the role of phonons in controlling coherence of polaritons.

3.3 Collective effects and dark state involvement

As has been described above, formation of polariton states in a large ensemble of molecules involves collective coherent superposition excitations from all the molecules. This leads to the formation of a large number of optically dark states that cannot be captured through linear spectroscopy because of their negligible oscillator strengths. Since the dark states can be excited to the upper polariton, we can directly observe the presence of ESA peaks from dark states[17] and with a large number of dark states we can see a stronger ESA signal. Thus simulating 2DES also will help us model the role of dark states in the energy transfer mechanisms of polaritonic states, which in turn can give us insight about how these dark

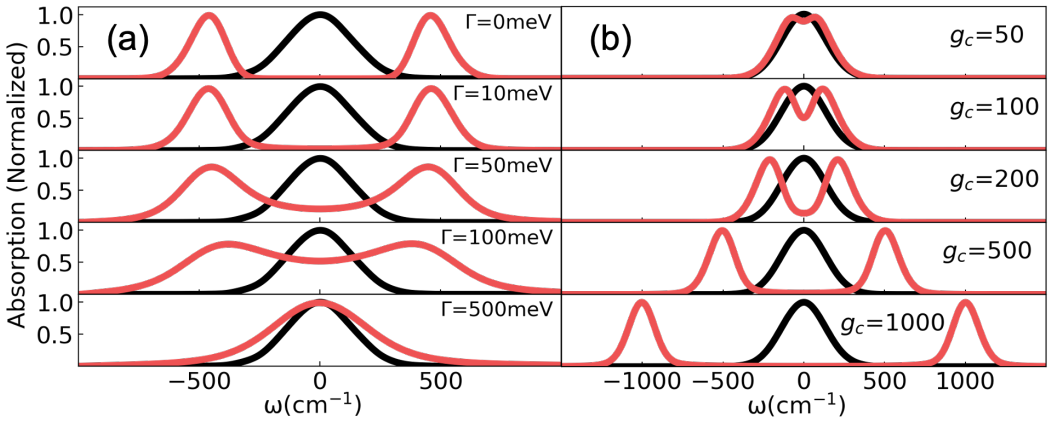

Figure 1: Linear absorption of monomer outside the cavity(black) and inside the cavity(red). (a) Variations in cavity loss rates with fixed coupling strength $\sim$ 456 cm^{-1}. (b) Varying cavity coupling strength (in cm^{-1}) with a fixed loss rate of Γ = 10meV.

states can be used for controlling chemical reactions and preserving coherent excitations.

4 Results

Here, I present the preliminary results from two different models, a monomer and a dimer placed inside a single cavity mode of various coupling strengths and loss rates. This helps us demonstrate the basic 2DES behavior of simple polaritonic systems.

4.1 Monomer coupled to cavity

The monomer is a single two-level system with an energy gap of 10,000 cm^{-1} and it is connected to 100 discretized bath oscillators causing a fluctuation in excitation energy. This is coupled to a single cavity mode of same energy (10,000 cm^{-1}).

Fig. 1a presents the linear absorption spectra of a monomer placed inside the cavity with varying loss rate at a fixed coupling strength of 456 cm^{-1}. The black background curve represents the bare monomer absoption. We can clearly see the Rabi splitting of lower and upper polariton peaks for a lossless cavity (Γ = 0 meV). Also, we can notice the reduced linewidth of the polariton peaks compared to those of the bare monomer because

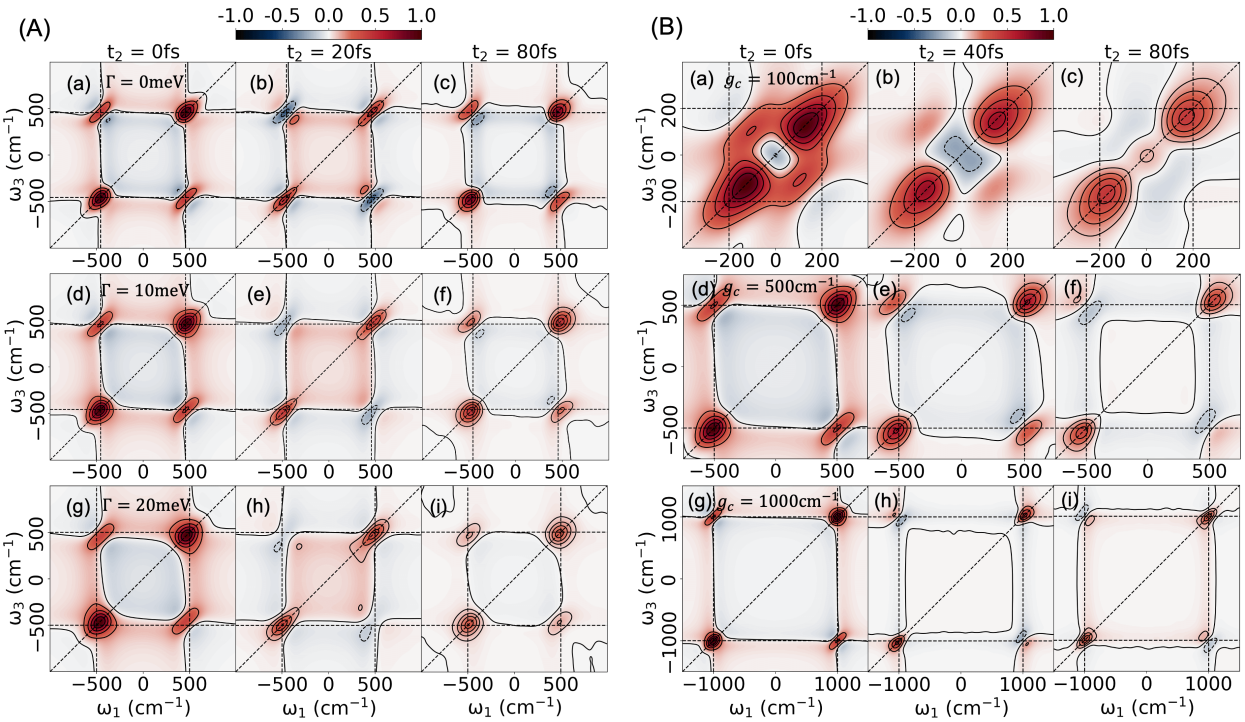

Figure 2: (A) shows purely absorptive 2DES for a monomer in cavity of (a)-(c)$\Gamma = 0$ meV, (d)-(f)$\Gamma = 10$ meV and (g)-(i)$\Gamma = 20$ meV at fixed $g_c = 57$meV with different waiting times t_2. (B) shows a purely absorptive 2DES for a monomer in cavity of (a)-(c)$g_c = 0$ meV, (d)-(f)$g_c = 10$ meV and (g)-(i)$g_c = 20$ meV at fixed loss of $\Gamma = 10$ meV with different waiting times t_2.

the monomeric bath is now shared equally by lower and upper polaritons, which effectively reduces the bath reorganization energy of the individual polaritons. With an increase of cavity loss rate, we see the broadening of polariton peaks which can be attributed to the additional photonic bath fluctuations. At very high loss rates, the matter can no longer coherently couple with the phtonic mode, and we do not see any Rabi splitting. In Fig. 1b, we vary g_c with fixed $\Gamma = 10$ meV. With an increase in g_c, we observe increased Rabi splitting.

Fig. 2A, shows the pure absorptive 2DES of the monomer paced in a cavity of varyinng loss rates. If we look at panel (a), we observe the Rabi splitting of peaks along them diagonal corresponding to upper and lower polaritons and also these peaks are elongated along the diagonal indicating their inhomogenous environment. We also see symmetric cross peaks which arise due to coupling between monomer and the cavity mode and is an indication of coherence between upper and lower polaritons. With time, we see oscillations in both

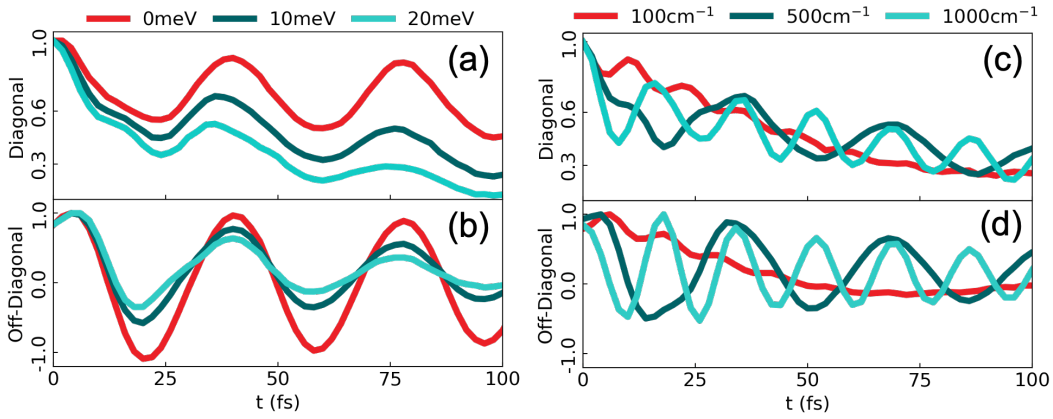

Figure 3: (a) and (b) shows decay (along t_2) in the upper diagonal peak and upper off-diagonal cross-peak intensity of a monomer coupled to the cavity at different loss rates for a fixed $g_c = 57$meV. (c) and (d) shows decay (along t_2) in the upper diagonal peak and the upper off-diagonal cross peak intensity of a monomer coupled to the cavity at different g_c for a fixed loss of $\Gamma = 10$meV.

the diagonal and cross-peak intensities as can be seen in the red curves of Fig. 3. These oscillations are evidence of coherent energy transfer mechanism between the polariton states. Now, if we keep increasing the cavity loss, we see a homogenous broadening of peaks (Fig. 2d - Fig. 2i). This is the result of the Lindbladian markovian treatment of cavity bath which results in a homogenous environment of the cavity mode. Also, we observe from the green and cyan curves in Fig. 3, that as we keep increasing the loss rate, the signal intensities decays faster and the coherence between lower and upper polaritons decay faster.

In Fig. 2B, we observe, with an increase in g_c, the Rabi splitting increases and from Fig 3c and Fig 3d, the coherent oscillations between upper and lower polariton states also increases.

4.2 Dimer coupled to cavity

We take a coupled molecular asymmetric dimer with an energy difference between exciton levels as $\epsilon_1 - \epsilon_2$ =100 cm^{-1} and there is an excitonic coupling of 100 cm^{-1}. Each monomer in the dimer has its own bath environment of 100 discretized bath modes. The molecular dipoles of each monomer are in the ratio $\mu_1/\mu_2 = -5$. We took a high reorganization energy for the bath modes such that the coherent process between the molecular excitons due to the

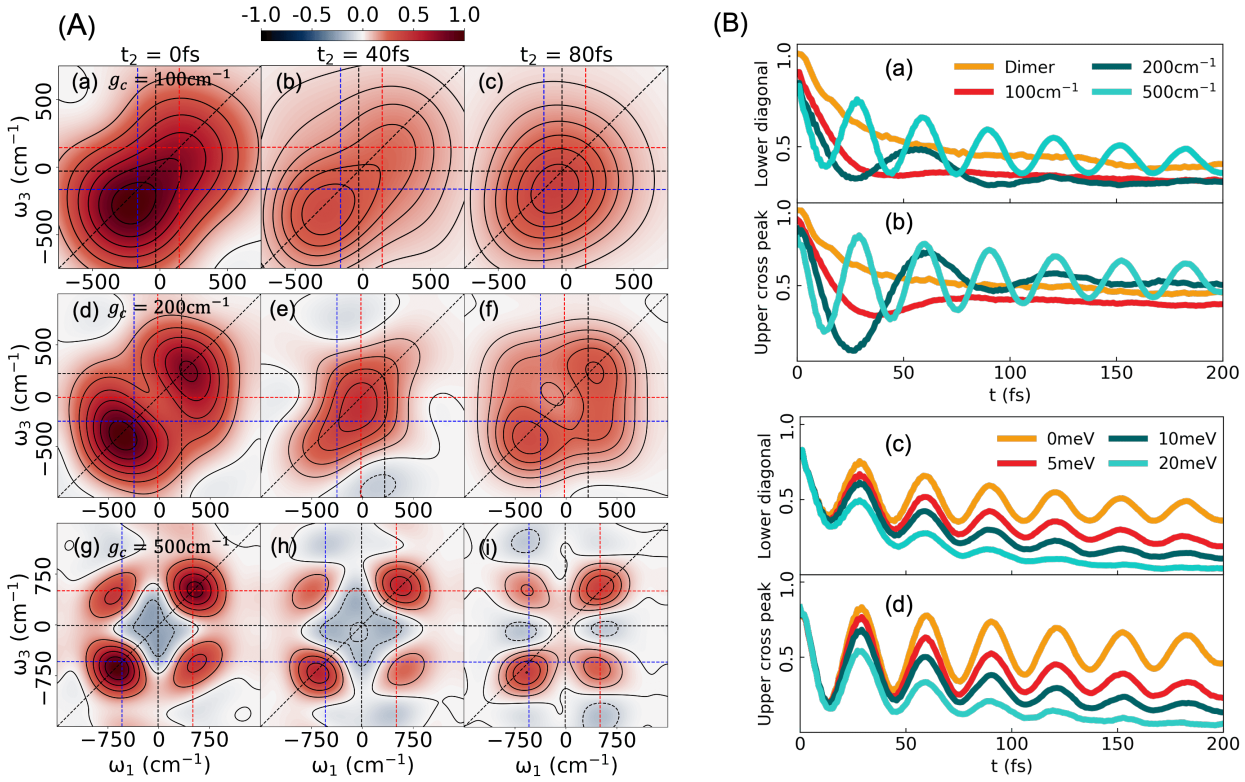

Figure 4: (a) and (b) shows decay (along t_2) in the upper diagonal peak and upper off-diagonal cross-peak intensity of a dimer coupled to the cavity at different g_c for a lossless cavity, Γ =0meV. (c) and (d) shows decay (along t_2) in the upper diagonal peak and the the upper off-diagonal cross peak intensity of a dimer coupled to the cavity at different Γ for a fixed $g_c = 500\text{cm}^{-1}$.

exciton coupling decays very fast.

Fig. 4A presents the 2DES of the dimer placed inside the cavity of varying coupling strengths. The high reorganization energy of bath cause a wide spread in the 2D spectra peaks, leading to mixing between different peaks and it becomes quite difficult for the low coupling regime to keep track of coherent cross-peaks. With increasing g_c, the lower and upper polariton peaks are more and more separated along the diagonals, and they become more coherent. Fig. 4B (a, b), we present the diagonal and off-diagonal peak intensity fluctuations of Fig. 4A. If we look just at the peak oscillations, we can now clearly see that in the dimer (yellow curve), the decoherence in the molecular system is very high, and we observe no coherent process between the molecular excitons. When placed inside the cavity, the scenario totally changes, and we start observing coherent oscillations in the system. Thus, the cavity

can be thought of as a source for introducing coherence in the system, and we can tune the cavity to overcome the internal dephasing processes of the system to preserve coherence for longer times. Fig. 4B (c, d), shows the peak oscillations of the dimer placed in cavity with $g_c = 500$ cm^{-1} at varying loss rates. We can clearly see that even with a high loss rate and a highly dephasing phonon environment, we can still preserve coherence lifetime of the polaritons upto 100's of femtoseconds.

5 Project goals

Based on the preliminary results that I have so far, the project can be expanded to some short-term goals and the ideas of these projects can also be directly extended to some long-term projects.

5.1 Short term goals

I am currently working on the submission of a paper describing the $\mathcal{L}$-PLDM method along with the preliminary results described above. With this method, the next steps in the following months will be to extend the code to simulate non-linear spectra of more molecules (at least 10) coupled to a cavity mode. This will be directly helpful in the two projects proposed above to simulate polaron decoupling and understanding the dark state mechanisms in polaritons. For the polaron decoupling project, I am currently testing different vibronic bath models that can be used to reproduce and explain the experimental 2DES of Ref.[7]. For the collective effect project, I am working with 10 monomeric molecules collectively coupled to a cavity mode with parameters similar to the monomer used in the preliminary results.

Along with this, the focus will also be on developing more efficient algorithms for non-linear spectra calculations. I also plan on using methods such as spin-PLDM combined with Lindblad to check the accuracy perspective of spectroscopy simulations.

5.2 Long term goals

A direct simple extension of the current project is the simulation of transient absorption (TA) spectroscopy for polaritons. Although TA contains less information than 2D spectroscopy and we can in principle take 2DES cross sections to get transient absorption signals, TA can also be used to probe polariton dynamics and obtain essential information[18]. Also, simulating TA should be much cheaper computationally compared to 2DES simulations. Thus, TA simulations can be feasible for large systems and can be very helpful in understanding processes like polariton transport.

Another extension of the current project is to simulate non-linear spectra in the IR regime and try to understand the polariton collective effects under Vibrational Strong Coupling (VSC)[19,20]. Coupling certain molecular vibrations with a cavity can help efficiently control ground state chemical reactions by either suppressing or enhancing reactivity along certain vibrations. These processes can be properly probed through 2DIR providing a clear mechanistic pathway of a ground state chemical reaction. Thus, it will be very interesting to develop simple models to explain fundamental insights of VSC rate modifications.

References

[1] J. A. Hutchison, T. Schwartz, C. Genet, E. Devaux, and T. W. Ebbesen, "Modifying chemical landscapes by coupling to vacuum fields," *Angew. Chem. Int. Ed.*, vol. 51, no. 7, pp. 1592–1596, 2012.

[2] M. Kowalewski and S. Mukamel, "Manipulating molecules with quantum light," *Proc. Natl. Acad. Sci. U.S.A.*, vol. 114, no. 13, pp. 3278–3280, 2017.

[3] J. Feist, J. Galego, and F. J. Garcia-Vidal, "Polaritonic chemistry with organic molecules," *ACS Photonics*, vol. 5, no. 1, pp. 205–216, 2018.

[4] R. F. Ribeiro, L. A. Martínez-Martínez, M. Du, J. Campos-Gonzalez-Angulo, and J. Yuen-

Zhou, "Polariton chemistry: controlling molecular dynamics with optical cavities," *Chem. Sci.*, vol. 9, no. 30, pp. 6325–6339, 2018.

[5] A. Thomas, L. Lethuillier-Karl, K. Nagarajan, R. M. Vergauwe, J. George, T. Chervy, A. Shalabney, E. Devaux, C. Genet, J. Moran, *et al.*, "Tilting a ground-state reactivity landscape by vibrational strong coupling," *Science*, vol. 363, no. 6427, pp. 615–619, 2019.

[6] F. Herrera and F. C. Spano, "Cavity-controlled chemistry in molecular ensembles," *Phys. Rev. Lett.*, vol. 116, no. 23, p. 238301, 2016.

[7] S. Takahashi and K. Watanabe, "Decoupling from a thermal bath via molecular polariton formation," *J. Phys. Chem. Lett.*, vol. 11, no. 4, pp. 1349–1356, 2020.

[8] A. Mandal, X. Li, and P. Huo, "Theory of vibrational polariton chemistry in the collective coupling regime," *J. Chem. Phys.*, vol. 156, no. 1, p. 014101, 2022.

[9] L. Valkunas, D. Abramavicius, and T. Mancal, *Molecular excitation dynamics and relaxation: quantum theory and spectroscopy*. John Wiley & Sons, 2013.

[10] M. Cho, *Two-dimensional optical spectroscopy*. CRC press, 2009.

[11] S. Mukamel, *Principles of nonlinear optical spectroscopy*. No. 6, Oxford University Press on Demand, 1999.

[12] P. Hamm, "Principles of nonlinear optical spectroscopy: A practical approach or: Mukamel for dummies," *University of Zurich*, vol. 41, no. 5, p. 77, 2005.

[13] J. Provazza, F. Segatta, M. Garavelli, and D. F. Coker, "Semiclassical path integral calculation of nonlinear optical spectroscopy," *J. Chem. Theory Comput.*, vol. 14, no. 2, pp. 856–866, 2018.

[14] P. Huo and D. F. Coker, "Communication: Partial linearized density matrix dynamics for dissipative, non-adiabatic quantum evolution," *J. Chem. Phys.*, vol. 135, no. 20, p. 201101, 2011.

[15] P. Huo and D. F. Coker, "Semi-classical path integral non-adiabatic dynamics: a partial linearized classical mapping hamiltonian approach," *Mol. Phys.*, vol. 110, no. 9-10, pp. 1035–1052, 2012.

[16] E. R. Koessler, A. Mandal, and P. Huo, "Incorporating lindblad decay dynamics into mixed quantum-classical simulations," *J. Chem. Phys.*, vol. 157, no. 6, p. 064101, 2022.

[17] M. Son, Z. T. Armstrong, R. T. Allen, A. Dhavamani, M. S. Arnold, and M. T. Zanni, "Energy cascades in donor-acceptor exciton-polaritons observed by ultrafast two-dimensional white-light spectroscopy," *Nat. Comm.*, vol. 13, no. 1, p. 7305, 2022.

[18] C. A. DelPo, B. Kudisch, K. H. Park, S.-U.-Z. Khan, F. Fassioli, D. Fausti, B. P. Rand, and G. D. Scholes, "Polariton transitions in femtosecond transient absorption studies of ultrastrong light–molecule coupling," *J. Phys. Chem. Lett.*, vol. 11, no. 7, pp. 2667–2674, 2020.

[19] T.-T. Chen, M. Du, Z. Yang, J. Yuen-Zhou, and W. Xiong, "Cavity-enabled enhancement of ultrafast intramolecular vibrational redistribution over pseudorotation," *Science*, vol. 378, no. 6621, pp. 790–794, 2022.

[20] W. Xiong, "Molecular vibrational polariton dynamics: What can polaritons do?," *Acc. Chem. Res.*, vol. 56, no. 7, pp. 776–786, 2023.